Communication

Pt(II)- and Pt(IV)-Bridged Cofacial Diporphyrins via Carbon#Transition Metal #-Bonds

Shigeru Yamaguchi, Taisuke Katoh, Hiroshi Shinokubo, and Atsuhiro Osuka

J. Am. Chem. Soc., **2008**, 130 (44), 14440-14441 • DOI: 10.1021/ja8066385 • Publication Date (Web): 09 October 2008

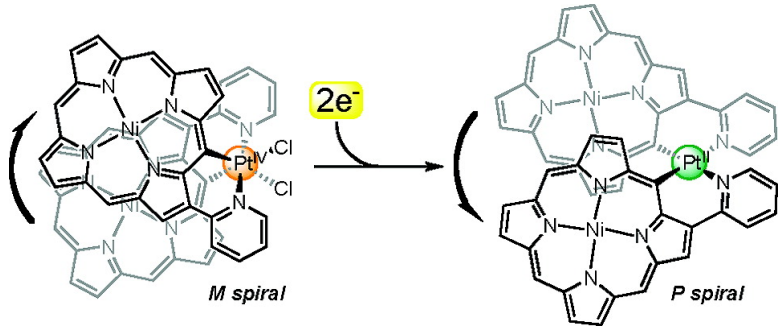

More About This Article

Additional resources and features associated with this article are available within the HTML version:

- Supporting Information
- Links to the 1 articles that cite this article, as of the time of this article download
- Access to high resolution figures
- Links to articles and content related to this article
- Copyright permission to reproduce figures and/or text from this article

View the Full Text HTML

J|A|C|S
COMMUNICATIONS

Published on Web 10/09/2008

Pt(II)- and Pt(IV)-Bridged Cofacial Diporphyrins via Carbon−Transition Metal σ-Bonds

Shigeru Yamaguchi, Taisuke Katoh, Hiroshi Shinokubo,* and Atsuhiro Osuka*

Department of Chemistry, Graduate School of Science, Kyoto University, Sakyo-ku, Kyoto 606-8502, Japan

Received August 25, 2008; E-mail: hshino@kuchem.kyoto-u.ac.jp; osuka@kuchem.kyoto-u.ac.jp

Cofacial diporphyrin architectures have attracted considerable attention due to their involvement in photosynthetic processes[1] as well as potential applications in recognition and activation of small molecules, sensing, and information storage.[2] Although various spacers have been invented for cofacial diporphyrins, there is no example of the directly metal-bridged cofacial diporphyrin system via metal−carbon σ-bonds. However, we envisioned the potential of redox-active transition metal spacers, which achieve the sensitivity toward external stimuli and the structural rigidity at the same time. Furthermore, tunable interactions of two porphyrins depending on the valence states of the metal bridge would be intriguing.

Metallated porphyrins at their peripheral positions have received much interest because of their rich properties, such as coordination, photophysical, and electrochemical properties. Among them, examples of porphyrins having transition metal−carbon σ-bond on their skeleton are still scarce.[3] The pioneering work of such a porphyrin has been reported by Arnold and co-workers. We have recently reported a novel class of ring metalated porphyrins, porphyrin pincer complexes.[4] Matano, Imahori, and co-workers reported β-M−C σ-bond bridged dimers of *meso*-phosphanyl porphyrin with a *trans*-configuration.[5] Here we wish to report the construction of a metal-bridged cofacial diporphyrin architecture through a cyclometalation strategy and their dynamic helical conformational change by reduction of the bridge.

The synthetic strategy of the Pt-bridged cofacial diporphyrin is shown in Scheme 1. As a ligand, β-pyridyl porphyrin **2** is synthesized from β-boryl porphyrin **1**[6] via a Suzuki−Miyaura cross-coupling reaction. The reaction of **2** with a Pt(IV) salt in toluene/AcOH at 100 °C, followed by repeated column chromatography, afforded **3** as an air and moisture stable brown solid in 7% yield along with **2** and unidentified products. Its parent ion peak was observed at m/z = 2245.9953 (calcd for $(C_{134}H_{148}N_{10}Ni_2PtCl)^+$ = 2245.9933 $[(M - Cl)^+]$) in its high resolution electrospray-ionization time-of-flight (HR ESI-TOF) mass spectrum. The ^{1}H NMR spectrum of **3** exhibits only one set of seven porphyrinic β-protons, suggesting the high symmetry of **3**. Notably, one β-proton H^1 (7.47 ppm) and *o*-protons of one aromatic substituent (6.17 and 5.63 ppm) show a substantial upfield shift, implying the cofacial geometry of **3**. Finally, the X-ray crystallographic analysis of **3** unambiguously elucidates the structure (Figures 1a and S8a). The porphyrin macrocycles take a ruffled conformation. Two porphyrin macrocycles are almost parallel (dihedral angle = 3° for 4N planes) and exhibit a large lateral shift (Ni−Ni distance = 5.15 Å). Close packing of two porphyrins was observed with an interporphyrinic distance of 3.4−3.8 Å for the 4N plane. The Pt coordination takes a distorted octahedral structure, in which the C−Pt−C angle is 82.5°. The UV/vis absorption spectrum broadens and splits due to exciton coupling. A substantial red shift of Q-bands is observed as well as broadening of the Soret band (Figure S7).

We then attempted reduction of the Pt(IV) bridge of **3** to Pt(II). To our delight, the reaction of **3** with an excess amount of

Scheme 1. Synthesis of Pt(IV)-Bridged Cofacial Diporphyrin **3** and Reduction of Pt(IV) Diporphyrin **3** to Pt(II) Diporphyrin **4**[a, b, c]

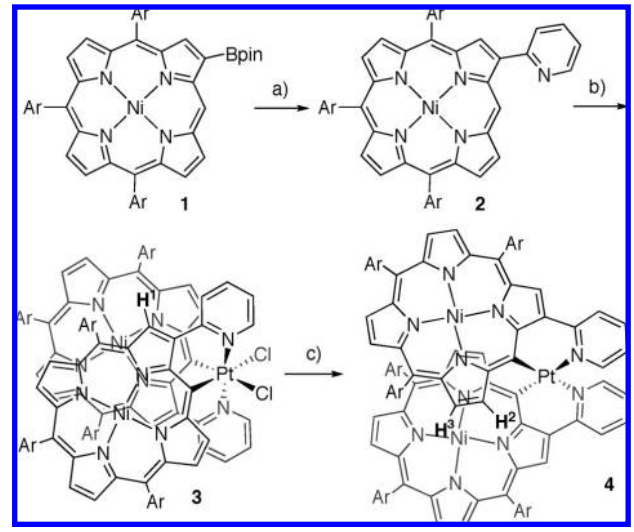

[a] 2-Iodopyridine, $Pd_2(dba)_3$, PPh_3, Cs_2CO_3, CsF, toluene/DMF/H_2O, reflux. [b] $(Bu_4N)_2PtCl_6$, toluene/AcOH, 100 °C. [c] $MeNHNH_2$, CH_2Cl_2, RT. Ar = 3,5-di-*tert*-butylphenyl, Bpin = 3,3,4,4-tetramethyl-2,5-dioxaboranyl.

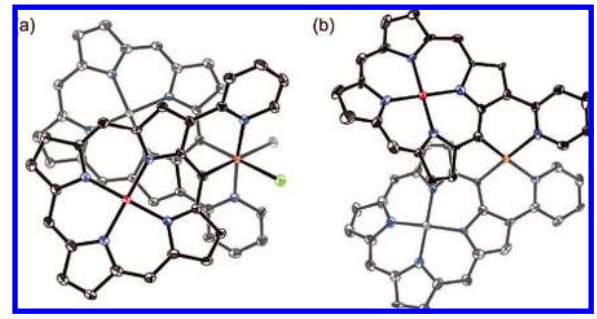

Figure 1. X-ray crystal structures. (a) Top views of **3** and (b) **4**. Hydrogen atoms and *meso*-aryl substituents are omitted for clarity. The thermal ellipsoids are scaled to the 50% probability level.

$MeNHNH_2$ in CH_2Cl_2 proceeded smoothly to furnish **4** in 65% yield, which was formed via a formal "slipping motion" of the two porphyrin macrocycles (Scheme 1).[7] HR ESI-TOF mass exhibited its parent ion peak at m/z = 2233.0161 (calcd for $(C_{134}H_{148}N_{10}Ni_2PtNa)^+$ = 2233.0151 $[(M + Na)^+]$). In the ^{1}H NMR, **4** also displays one set of proton peaks of porphyrin macrocycles. The doublet signal of β-protons H^2 and H^3 of **4** appeared in the upfield region (6.97 and 6.52 ppm), while the singlet peak of H^1 of **3** was upfield shifted. These changes clearly indicate the lateral slipping motion from Pt(IV)-dimer **3** to Pt(II)-dimer **4**. Finally, the cofacial porphyrin geometry of **4** was confirmed by X-ray crystallographic analysis (Figures 1b and S8b). The coordination of the Pt(II) center

10.1021/ja8066385 CCC: $40.75

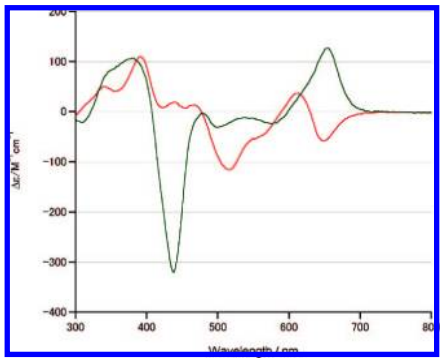

Figure 2. CD spectra of **3*M*** (red) and **4*P*** (green).

is square planar. The length of C−Pt bonds of **4** is 1.993 Å, which is shorter than that of **3** (2.044 Å). The two porphyrin macrocycles stand somewhat apart from each other (dihedral angle = 35.4° for 4N planes and Ni−Ni distance = 7.208 Å) in comparison to the overlapped structure of **3**. The macrocycles also take a ruffled conformation, and the averages of the mean plane deviations of **3** and **4** are almost the same (**3**, 0.314 Å and **4**, 0.323 Å for 4N plane). The UV/vis absorption spectrum of **4** shows broadening, splitting, and a red shift ($\Delta\lambda$ = 15 nm for the Soret band as compared to **2**, Figure S7).

These Pt-bridged cofacial diporphyrins **3** and **4** have inherent helical chirality. We succeeded to separate all the enantiomers by the chiral HPLC. The CD spectra of enantiomers exhibit distinct Cotton effects which are unpredictable by the empirical method (Figures 2 and S11).[8] No racemization of enantiomers was observed in both the solid states and solution at least for 1 month. This stability is probably due to the bulkiness of the porphyrin as well as robust Pt−C and Pt−N bonds. Furthermore, we found helicity inversion by reduction of enantiomers: reduction of *M* spiral of **3** (**3*M***) predominantly yielded one enantiomer of **4** (**4*P***) in 77% ee.[9] The CD pattern of **4*P*** matches well with the calculated spectrum by the TD-DFT method (Figure S15).

The electronic coupling of the porphyrin moieties of **3** and **4** was examined by cyclic voltammetry along with **2** (Figure S11, V vs ferrocene/ferrocenium ion pair).[10] Pt(II)-bridged dimer **4** shows distinct splitting of the first oxidation potential: the reversible waves were observed at 0.13 and 0.36 V as one-electron processes and at 0.72 V as a two-electron process. In sharp contrast, two reversible waves were observed at 0.33 and 0.67 V for Pt(IV)-bridged dimer **3**. This different behavior highlights the importance of the oxidation state of the Pt-bridge and thus involvement of d-orbitals in the interporphyrinic interaction. The lower potential of **4** than that of **2** (E_{ox1} = 0.48 V) is mainly due to the electron-donating character of the Pt(II) atom.[11] In addition, the first oxidation potential of **3** is higher than that of **4** because of less electron-donating ability of Pt(IV) as compared to Pt(II). The square planar Pt(II) center has a nonbonding d_{z^2} orbital, and a radical cation on one porphyrin can be delocalized by the donation of the d-electron. DFT calculations support involvement of the d_{z^2} orbital to the HOMO of **4** (Figure S14). Further investigation on the electrochemical behavior is currently underway.[12]

In conclusion, we have achieved the synthesis of Pt(IV)- and Pt(II)-bridged cofacial diporphyrins. Both platinum centers force two porphyrin macrocycles to be in close proximity by the stable two Pt−C σ-bonds supported by the pyridyl groups. At the same time, the platinum bridge offers a conformationally flexible nature to the complexes due to the susceptibility of platinum toward redox reaction. These complexes also exhibit helical chirality. We are now focusing on the applications of these Pt-bridged cofacial diporphyrins in asymmetric catalysis and material science.

Acknowledgment. This work was supported by Grants-in-Aid for Scientific Research (Nos. 18685013 and 20037034) from MEXT, Japan. S.Y. appreciates the JSPS Research Fellowships for Young Scientists. We also thank Prof. Hitoshi Tamiaki (Ritsumeikan Univ.) for CD measurement.

Supporting Information Available: General procedures, spectral data for compounds and absorption spectra. CIF files for the X-ray analysis of **3**, **3*M***, and **4**. This material is available free of charge via the Internet at http://pubs.acs.org.

References

(1) (a) Deisenhofer, J.; Epp, O.; Miki, K.; Huber, R.; Michel, H. *J. Mol. Biol.* **1984**, *180*, 385. (b) Huber, R. *Angew. Chem., Int. Ed. Engl.* **1989**, *28*, 848.
(2) (a) Pognon, G.; Boudin, C.; Schenk, K. J.; Bonin, M.; Bach, B.; Weiss, J. *J. Am. Chem. Soc.* **2006**, *128*, 3488–3489. (b) Cui, W.; Zhang, X. P.; Wayland, B. B. *J. Am. Chem. Soc.* **2003**, *125*, 4994. (c) Yagi, S.; Ezoe, M.; Yonekura, I.; Takagishi, T.; Nakazumi, H. *J. Am. Chem. Soc.* **2003**, *125*, 4068. (d) Rosenthal, J.; Luckett, T. D.; Hodgkiss, J. M.; Nocera, D. G. *J. Am. Chem. Soc.* **2006**, *128*, 6546. (e) Proni, G.; Oesticelli, G.; Huang, X.; Quraishi, N.; Nakanishi, K.; Berova, N. *Chem. Commun.* **2002**, 1590. (f) Shinkai, S.; Ikeda, M.; Sugasaki, A.; Takeuchi, M. *Acc. Chem. Res.* **2001**, *34*, 494.
(3) (a) Smith, K. M.; Langry, K. C.; Minnetian, O. M. *J. Org. Chem.* **1984**, *49*, 4602. (b) Arnold, D. P.; Sakata, Y.; Sugiura, K.; Worthington, E. I. *Chem. Commun.* **1998**, *n/a*, 2331. (c) Hartnell, R. D.; Arnold, D. P. *Organometallics* **2004**, *23*, 391. (d) Hartnell, R. D.; Arnold, D. P. *Eur. J. Inorg. Chem.* **2004**, 1262. (e) Hodgson, M. J.; Healy, P. C.; Williams, M. L.; Arnold, D. P. *J. Chem. Soc., Dalton Trans.* **2002**, 4497. (f) Arnold, D. P.; Healy, P. C.; Hodgson, M. J.; Williams, M. L. *J. Organomet. Chem.* **2000**, *607*, 41.
(4) Yamaguchi, S.; Katoh, T.; Shinokubo, H.; Osuka, A. *J. Am. Chem. Soc.* **2007**, *129*, 6392.
(5) Matano, Y.; Matsumoto, K.; Nakano, Y.; Uno, H.; Sakaki, S.; Imahori, H. *J. Am. Chem. Soc.* **2008**, *130*, 4588.
(6) Hata, H.; Shinokubo, H.; Osuka, A. *J. Am. Chem. Soc.* **2005**, *127*, 8264.
(7) The reaction of **3** with $NaBH_4$ afforded **4** in 20% yield with lower selectivity. We attempted the oxidation of **4** to **3** (oxidants: $FeCl_3$, $CuCl_2$, $NaAuCl_4$ and so on), which resulted in no reaction or decomposition of **4**.
(8) For examples, see: Muranaka, A.; Asano, Y.; Tsuda, A.; Osuka, A.; Kobayashi, N. *ChemPhysChem* **2006**, *7*, 1235, and references therein.
(9) For other examples of helicity inversion by redox stimuli, see: Zahn, S.; Canary, W. J. *Science* **2000**, *288*, 1404, and references therein.
(10) E_{ox1} of **2** was determined by differential pulse voltammetry because of existence of the reactive pyridyl group and free *meso*-position. For electrochemical reaction of pyridine derivatives with porphyrins, see: Ruhlmann, L.; Lobstein, S.; Gross, M.; Giraudeau, A. *J. Org. Chem.* **1999**, *64*, 1352.
(11) The DFT calculation indicates that **2** also takes a ruffled conformation (Figure S16). The structural difference in macrocycles between **2** and **4** only slightly influences the difference of the oxidation potentials.
(12) The reason is not clear why **3** shows only two waves despite the close proximity of two porphyrins. The reduction waves for **4** have not been fully characterized due to their complicated features.

JA8066385